Membrane-based acoustic metamaterial with near-zero refractive index*

Yi-Feng Li(李义丰)[1,2,†], Jun Lan(蓝君)[1], Hui-Yang Yu(余辉洋)[1], Xiao-Zhou Liu(刘晓宙)[3], and Jia-Shu Zhang(张嘉澍)[4]

[1] *Department of Computer Science and Technology, Nanjing Tech. University, Nanjing* 211800, *China*
[2] *Key Laboratory of Modern Acoustics, Ministry of Education, Nanjing University, Nanjing* 210093, *China*
[3] *Key Laboratory of Modern Acoustics, Ministry of Education, Institute of Acoustics and School of Physics, Nanjing University, Nanjing* 210093, *China*
[4] *Department of Electronic and Electrical Engineering, The University of Sheffield, Sheffield S*102*TN, UK*

(Received 12 August 2016; revised manuscript received 10 October 2016; published online 29 November 2016)

We investigate a one-dimensional acoustic metamaterial with a refractive index of near zero (RINZ) using an array of very thin elastic membranes located along a narrow waveguide pipe. The characteristics of the effective density, refractive index, and phase velocity of the metamaterial indicate that, at the resonant frequency f_m, the metamaterial has zero mass density and a phase transmission that is nearly uniform. We present a mechanism for dramatic acoustic energy squeezing and anomalous acoustic transmission by connecting the metamaterial to a normal waveguide with a larger cross-section. It is shown that at a specific frequency f_1, transmission enhancement and energy squeezing are achieved despite the strong geometrical mismatch between the metamaterial and the normal waveguide. Moreover, to confirm the energy transfer properties, the acoustic pressure distribution, acoustic wave reflection coefficient, and energy transmission coefficient are also calculated. These results prove that the RINZ metamaterial provides a new design method for acoustic energy squeezing, super coupling, wave front transformation, and acoustic wave filtering.

Keywords: acoustic metamaterial, refractive index of near zero (RINZ), energy squeezing, transmission enhancement

PACS: 43.35.+d, 43.20.+g, 68.60.Bs **DOI:** 10.1088/1674-1056/26/1/014302

1. Introduction

Acoustic metamaterials are broadly defined as artificial composite materials that can freely manipulate their constituent parameters, such as mass density ρ and bulk modulus B. For instance, acoustic metamaterials with extreme positive, negative, or near-zero parameters can be achieved with different types of structures. In previous studies, a kind of tubular acoustic metamaterial with negative density was constructed using an array of membranes.[1,2] The negative bulk modulus metamaterials were fabricated based on periodically distributed Helmholtz resonators (HRs)[3–5] or side holes.[6,7] Double negative (DNG) metamaterials have been designed by mixing two structures that have independent negative bulk modulus and negative mass density.[8–10] These acoustic metamaterials have potential applications in insulating broadband frequency noise,[11] tunable acoustic radiation patterns,[12] and acoustic invisible cloaking.[13–15]

Recently, the class of metamaterials that has a refractive index of near zero (RINZ) has become an important topic because of their anomalous properties in wave propagation. In an electromagnetic field, a RINZ metamaterial indicates that the medium has the characteristics of an infinitely large phase velocity and zero phase delay. These remarkable properties can be used for applications such as electromagnetic energy squeezing,[16] phase coupling,[17,18] and transparency/cloaking devices.[19,20] In principle, electromagnetic metamaterial research methods are also suitable for acoustic metamaterials. Although research into acoustic metamaterials has focused on the properties of negative mass density and/or negative bulk modulus, recent research on RINZ acoustic metamaterials has drawn considerable attention. To obtain RINZ acoustic metamaterials, the effective bulk modulus $B_{\rm eff}$ should be infinite or the effective mass density $\rho_{\rm eff}$ should be equal to zero. To manipulate the value of B accordingly, methods using an array of HRs[21] or side holes[22] have been proposed for one-dimensional (1D) acoustic metamaterials. To make ρ equal to zero, methods using membranes have been discussed for 1D[23,24] and two-dimensional (2D)[25] RINZ acoustic metamaterials. Depending on the working frequency, the methods mentioned above can make the refractive index n of the metamaterial near zero, imaginary, or positive.

In this paper, we present a 1D membrane-based RINZ acoustic metamaterial that has a near zero effective mass density around the resonant frequency of the system. The effective density, refractive index, and phase velocity of the acoustic metamaterial are derived by introducing the concept of hid-

*Project supported by the National Natural Science Foundation of China (Grant Nos. 61571222, 11104142, and 11474160), the Natural Science Foundation of Jiangsu Province, China (Grant No. BK20161009), the Qing Lan Project of Jiangsu Province, China, and the Six Talent Peaks Project of Jiangsu Province, China.

†Corresponding author. E-mail: lyffz4637@163.com

den force, which has been discussed for analogue mechanical systems.[26] To investigate the energy squeezing, transmission enhancement, and super coupling properties of the RINZ metamaterial, a normal waveguide material with a bigger cross-sectional area is directly coupled at the right end of the metamaterial. Using acoustic transmission line theory and fluid impedance theory, we discuss the properties of acoustic energy transmission and acoustic pressure distribution. In addition, numerical finite element method (FEM) simulations are performed to test and demonstrate the energy squeezing, transmission enhancement, and super coupling phenomena through the acoustic metamaterial. The results show that, at the resonant frequency $f_{\rm m}$, the phase is almost uniform (super coupling) along the metamaterial, and at the specific frequency f_1 (which is slightly larger than $f_{\rm m}$), zero reflection, energy squeezing, and high transmission are achieved despite the large geometric mismatch at the interface of the two materials. Such anomalous acoustic characteristics are mainly inspired by the metamaterial with near zero mass density.

2. Membrane-based RINZ metamaterials

The structure of a 1D RINZ acoustic metamaterial is schematically shown in Fig. 1(a). The metamaterial consists of an array of very thin elastic membranes ($\rm M_{\it i}$) located along a waveguide pipe. The length of each unit cell and the inner diameter of the waveguide are $L = 70$ mm and $l = 30$ mm, respectively, as shown in Fig. 1(b). The tension of the membrane is $\tau = 20\ \rm N{\cdot}m^{-1}$. A sound source and an absorber are located at both ends of the metamaterial to generate and absorb acoustic waves, thus preventing reflection from the end of the metamaterial. As the wavelength is much longer than the periodic distance between the two adjacent membranes ($L \ll \lambda$), this acoustic metamaterial can be regarded as a homogenized medium.[4]

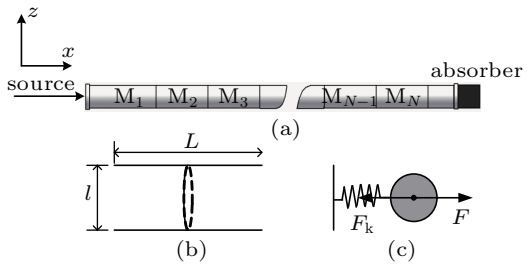

Fig. 1. (a) Model of a one-dimension (1D) membrane-based RINZ acoustic metamaterial. (b) The picture and dimensions of a single unit cell. (c) The equivalent mechanic prototype of a unit cell.

2.1. Refractive index and phase velocity

A mechanics-based concept can be used to describe the propagation of acoustic waves in this acoustic metamaterial, as recently demonstrated by Lee *et al.*[26] In this study, when an acoustic wave is transmitted into a waveguide, the center of the membrane in a unit cell of the acoustic metamaterial is subject to two forces, the applied force and the hidden force. The applied force $F = \Delta p s_{\rm m}$ originates from the two adjacent unit cells, where Δp and $s_{\rm m}$ are the pressure difference across the unit cell and the cross-sectional area of the waveguide (or the area of the membrane), respectively. The hidden force $F_{\rm k} = -k_{\rm m}\xi$ stems from the membrane's spring-like properties, where $k_{\rm m}{=}8\pi\tau$ and ξ are the effective stiffness of the membrane and the displacement of the center of the membrane, respectively. In general, once the applied force impacts the membrane, the hidden force generates and acts on the membrane. These two forces are collinear, the equivalent mechanical prototype of a unit cell is shown in Fig. 1(c). According to Newton's law, the motion equation of a unit cell is $M\ddot{\xi} + k_{\rm m}\xi = F$, where $M = \rho_0 s_{\rm m} L + M_{\rm m}$ is the mass of a unit cell. Here, $\rho_0 = 1.21\ \rm kg/m^3$ and $M_{\rm m} = 2$ mg are the density of air and the mass of the membrane, respectively. Hence, the effective mass of a unit cell can be obtained as $M_{\rm eff} = M/(1 + F_{\rm k}/F)$. Using the displacement harmonic function $\xi = \xi_0 \exp(-{\rm j}\omega t)$, the effective mass of a unit cell can be expressed as

$$M_{\rm eff} = M\left(1 - \frac{\omega_{\rm m}^2}{\omega^2}\right), \tag{1}$$

where $\omega_{\rm m} = \sqrt{k_{\rm m}/M}$ is the resonant angular frequency. It can be seen from Eq. (1) that, as the frequency increases through $\omega_{\rm m}$, the value of $M_{\rm eff}$ makes a sharp transition from negative to positive. As the acoustic metamaterial can be regarded as a homogenized medium, the effective mass density can be defined by $\rho_{\rm eff} = M_{\rm eff}/V$, where $V = s_{\rm m}L$ is the volume of the unit cell. Therefore,

$$\rho_{\rm eff} = \rho'\left(1 - \frac{\omega_{\rm m}^2}{\omega^2}\right), \tag{2}$$

where the average density of membrane-loaded air $\rho' = M/V$ ($\approx 1.25\ \rm kg/m^3$) is a constant that is slightly greater than the density of air ρ_0. This equation shows that the metamaterial exhibits negative effective mass density from zero frequency to the resonant frequency $\omega_{\rm m}$, which provides a wide low-frequency forbidden band (LFB). The other constituent parameter for acoustic metamaterials is the effective modulus $B_{\rm eff}$. According to the pressure–volume relation, the existence of membranes does not change the effective modulus of this acoustic metamaterial, so $B_{\rm eff} = B_0$,[1,26] where B_0 (1.42×10^5 Pa) is the bulk modulus of air. For this system, the refractive index can be defined as the ratio of the phase velocity in free space to that in the acoustic metamaterial, i.e., $n = v_0/v_{\rm a}$, where $v_0 = 1/\sqrt{\rho' B_0^{-1}}$ and $v_{\rm a} = \sqrt{B_{\rm eff}/\rho_{\rm eff}} = \sqrt{B_0/\rho'(1 - \omega_{\rm m}^2/\omega^2)}$. Therefore,

$$n = v_0\sqrt{\frac{\rho'(1 - \omega_{\rm m}^2/\omega^2)}{B_0}}. \tag{3}$$

The effective density, phase velocity, and refractive index of the acoustic metamaterial with respect to frequency are

shown in Figs. 2(a)–2(c), respectively. In the frequency range $f < f_m$ ($f_m = \omega_m/2\pi$), the effective density ρ_{eff} is negative. Thus, the refractive index and the phase velocity are imaginary. In this situation, the acoustic metamaterial works in a forbidden band and can be used for the absorption of noise. In the frequency range $f > f_m$, we observe that the effective density, phase velocity, and refractive index are all positive, and an increase in the frequency causes the phase velocity to decrease continuously until it is equal to v_0. Hence, in this frequency domain, the acoustic waves propagate well in the metamaterial. When the frequency is close to the resonant frequency f_m, the effective density and refractive index simultaneously converge to zero. Notably, the phase velocity is very large and tends to infinity near the resonant frequency f_m. These results indicate that the acoustic metamaterial has potential applications as an acoustic wave filter and wave front transformer.

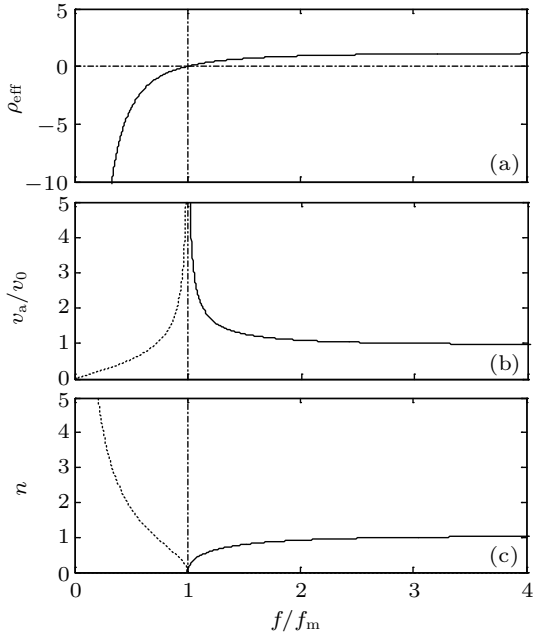

Fig. 2. (a) Effective density, (b) phase velocity and (c) refractive index are plotted versus frequency. In panels (b) and (c), the solid and broken curves stand for the real and image part, respectively. Significant properties occur at the frequency $f/f_m = 1$.

To confirm the preceding analytical results, we simulated the propagation of acoustic waves in the 1D RINZ acoustic metamaterial by FEM. In theory, the length of the acoustic metamaterial does not change the space distribution characteristics of the pressure field. Thus, for convenience, we selected an acoustic metamaterial with 20 unit cells for this calculation. In the FEM simulation, the membrane was considered as an additional acoustic impedance $z_m = 1/j\omega c_m$, where $c_m = s_m^2/k_m$. Along the x-direction, a plane acoustic wave with an amplitude of 1 Pa enters the left inlet of the waveguide. Figure 3 shows the distribution of the pressure field in the acoustic metamaterial at frequencies of 250, 453.7, and 900 Hz, which are below, equal to, and above the resonant frequency f_m, respectively. From Fig. 3(a), we can see that if the frequency of the incident wave is below f_m, the acoustic wave can only penetrate into the first few units. This is because, in the frequency range $f < f_m$, the effective mass density ρ_{eff} is negative, and the phase velocity and refractive index are imaginary. In this case, the metamaterial is opaque, and most of the incident energy is reflected back to the source. When the frequency of the incident wave is equal to the resonant frequency f_m, the effective density and the refractive index are near zero, as shown in Fig. 3(b). In this case, the wave can transmit through all the metamaterial units and the distribution of the pressure field is nearly constant, which means that the phase is nearly uniform in the RINZ metamaterial. Therefore, this RINZ metamaterial can be used as a phase super coupler. Figure 3(c) shows the acoustic pressure distribution in the metamaterial at a frequency of 900 Hz. At this frequency, the effective density and refractive index are positive and the metamaterial is transparent. The FEM results are consistent with the preceding analysis obtained using the mechanics-based concept (see Fig. 2).

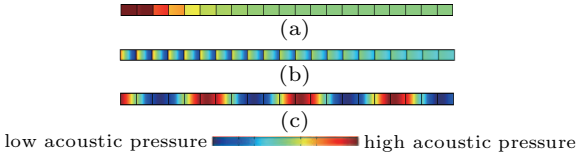

Fig. 3. (color online) FEM simulation results of the acoustic pressure field in the RINZ acoustic metamaterial, at the frequency (a) below, (b) equal to, and (c) above the resonant frequency f_m.

2.2. Acoustic reflection and energy transmission coefficients

In this section, we theoretically analyze the transmission properties of an acoustic wave from the RINZ acoustic metamaterial to a normal waveguide material that has a large cross-sectional area and is directly connected to the metamaterial. The composite structure of the system is shown in Fig. 4(a), where the normal waveguide material of length 3 m and radius 45 mm is terminated by the absorber. The geometric structure of the metamaterial is the same as that shown in Fig. 1(a), with a length of 7 m. At the interface of the two materials, the cross-section suddenly changes and the impedances of each material are different. Figure 4(b) shows a schematic of the cross-section of the two materials, in which $p_i = p_{ai}\exp(jk(x-7))$ is the incident wave and $p_r = p_{ar}\exp(-jk(x-7))$ is the reflected wave in the metamaterial, $p_t = p_{at}\exp(jk_n(x-7))$ is the transmitted wave in the normal material, where p_{ai}, p_{ar}, and p_{at} are the incident, reflected, and transmitted waves at the interface, respectively. Here, k and k_n are the wave vectors for the metamaterial and the normal material, respectively. According to acoustic transmission line theory and fluid impedance theory,[3] the impedance relation between the sides of each membrane can be given by

$$z_{al} = z\frac{z_{ar} + jz\tan kL}{z + jz_{ar}\tan kL}, \tag{4}$$

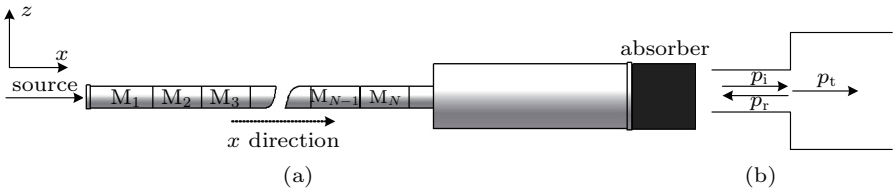

Fig. 4. (a) Composite structure and (b) schematic of the cross-section of the RINZ metamaterial and the normal material.

where z_{al} and z_{ar} are the impedances of the fluids on the left and right of the membrane, respectively, and z is the distributed impedance of the waveguide. The impedance relation between the membrane and the fluid in the waveguide can be expressed as

$$z_{al} = z_{ar} + z_m. \tag{5}$$

Applying Eqs. (4) and (5) recursively N times, the impedance z_M of the acoustic metamaterial with N unit cells can be obtained. Based on the acoustic boundary condition, the acoustic pressure and volume velocity are simultaneously continuous at the interface ($x = 7$ m) between the two materials. This gives the following equations:

$$\begin{cases} p_{ai} + p_{ar} = p_{at}, \\ s_m\,(p_{ai}/z_M - p_{ar}/z_M) = s_n p_{at}/z_n, \end{cases} \tag{6}$$

where s_n is the cross-sectional area of the normal material and $z_n = \rho_0 v_0$ is the impedance of the medium in the normal material. By combining the two parts of Eq. (6), the acoustic pressure reflection coefficient r_p and transmission coefficient t_p at the interface of the two materials can be written as

$$r_p = \frac{p_{ar}}{p_{ai}} = \frac{(z_n/s_n - z_M/s_m)}{(z_M/s_m + z_n/s_n)}, \tag{7}$$

$$t_p = \frac{p_{at}}{p_{ai}} = \frac{2z_n/s_n}{(z_M/s_m + z_n/s_n)}. \tag{8}$$

Equations (7) and (8) show that the parameters determining the acoustic pressure reflection and transmission coefficients at the interface of the two different media are the acoustic impedance z_M/s_m and z_n/s_n, rather than the characteristic impedances z_M and z_n.[21,27] Furthermore, it can be seen from Eq. (7) that there exist two critical frequency points. The first corresponds to the case $z_M = 0$, where the effective density ρ_{eff}=0, the reflection coefficient is 1, and the acoustic wave is completely reflected. The second frequency point corresponds to the situation in which the acoustic impedances between the metamaterial and the normal material are matched, i.e., $z_M/s_m = z_n/s_n$, which indicates that the reflection coefficient is zero and the acoustic wave realizes non-reflection transmission. Figure 5(a) shows the acoustic wave reflection from the normal material to the metamaterial with respect to the frequency given by Eq. (7). At the lower frequencies of $f \le f_m$, the reflection coefficient is near 1 and the almost acoustic waves are reflected to the source; thus, the metamaterial is opaque and no waves can propagate into the normal material. When the frequency is 465 Hz ($= f_1$), the reflection coefficient becomes zero, as shown in the magnified part of Fig. 5(a). This means that the acoustic impedances of the two materials are matched and the acoustic waves are totally transmitted. The value of f_1 is slightly larger than f_m, as shown in Fig. 2(a). At frequency f_1, the effective density of the metamaterial is close to zero. We can predict that if $s_n \gg s_m$, the two frequencies f_1 and f_m will be exactly the same, because in this situation the large difference in cross-sectional area at the connection compensates for the mismatch between the acoustic impedance at a frequency of f_m, which leads to the total transmission associated with the uniform phase along the metamaterial. In the frequency range $f > f_1$, the composite system is transparent and the wave can propagate from the metamaterial to the normal material. As the cross-sectional area of the normal material is nine times that of the metamaterial, i.e., $s_n = 9s_m$, the interface of the two materials can be regarded as a soft boundary, and in this case the calculated reflection coefficient is negative. The energy transmission coefficient can be defined as $T_{energy} = (1 - |r_p|^2)s_m v_a/s_n v_0$. The evolution of T_{energy} with respect to frequency is plotted in Fig. 5(b), where we can see that the energy transmission is sensitive to the frequency. At the specific frequency f_1, it is indeed possible to achieve total energy transmission, despite the strong geometrical mismatch between the metamaterial and the normal material. This is the result of acoustic impedance matching between the two materials in the RINZ condition. Consequently, the acoustic wave provides a unique capability of high transmission through the RINZ metamaterial.

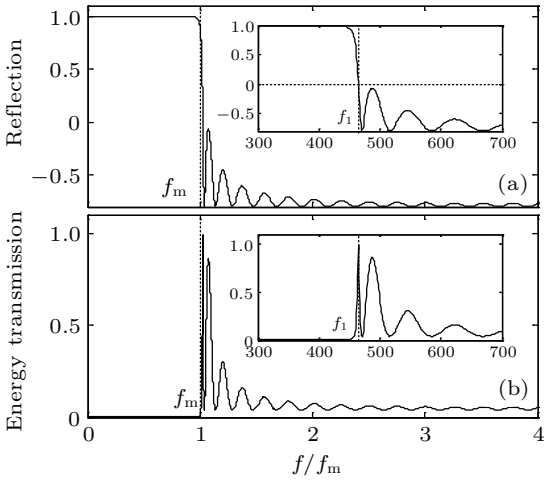

Fig. 5. (a) Acoustic reflection and (b) energy transmission coefficients of the composite system with respect to the normalized frequency f/f_m.

2.3. Acoustic wave propagation characteristics

We now investigate the acoustic wave propagation characteristics for various transmission distances from the RINZ acoustic metamaterial to the normal material. In our structure, for a monochromatic forward traveling acoustic wave, the acoustic pressure in the RINZ acoustic metamaterial can be expressed as

$$p_{\mathrm{m}}(x) = p_{\mathrm{ai}}^{\mathrm{e}}\,\mathrm{e}^{\mathrm{j}kx} + p_{\mathrm{ar}}^{\mathrm{e}}\,\mathrm{e}^{-\mathrm{j}kx}, \tag{9}$$

where $p_{\mathrm{ai}}^{\mathrm{e}}$ and $p_{\mathrm{ar}}^{\mathrm{e}}$ are the amplitudes of the incident and reflected acoustic pressures at the left entrance to the acoustic metamaterial. $p_{\mathrm{ai}}^{\mathrm{e}}$ can be determined by the initial condition, and we assume $p_{\mathrm{ai}}^{\mathrm{e}} = 1$ Pa. According to Eq. (7), $p_{\mathrm{ar}}^{\mathrm{e}}$ can be calculated using the relation $p_{\mathrm{ar}}^{\mathrm{e}} = p_{\mathrm{ar}}\exp(\mathrm{j}7k) = r_{\mathrm{p}}p_{\mathrm{ai}}\exp(\mathrm{j}7k)$, where k is the wave vector of the metamaterial given by $k = \omega\sqrt{\rho_{\mathrm{eff}}/B_0} = \sqrt{\rho'\omega^2 - \omega_{\mathrm{m}}^2/B_0}$. In the case $\omega \geq \omega_{\mathrm{m}}$, k is a real number, and the acoustic wave propagates in the x-direction without attenuation. The acoustic energy moves in the same direction away from the source, and the incident acoustic pressure at the interface is given by $p_{\mathrm{ai}} = p_{\mathrm{ai}}^{\mathrm{e}} = 1$ Pa. However, when $\omega < \omega_{\mathrm{m}}$, the wave vector k is an imaginary number, and the wave attenuates in the x-direction rapidly and cannot propagate. The sound energy moves in the negative x-direction toward the source, and the incident acoustic pressure at the interface is $p_{\mathrm{ai}} = 0$. To explain this characteristic explicitly, when $\omega < \omega_{\mathrm{m}}$, Eq. (9) can be simplified as

$$p_{\mathrm{m}}(x) = p_{\mathrm{ai}}^{\mathrm{e}}\,\mathrm{e}^{-k_1 x} + p_{\mathrm{ar}}^{\mathrm{e}}\,\mathrm{e}^{k_1 x}, \tag{10}$$

where the wave vector k_1 is given by $k_1 = \sqrt{\rho'(\omega_{\mathrm{m}}^2 - \omega^2)/B_0}$. Equations (9) and (10) express the acoustic pressure in the acoustic metamaterial. According to the definition of the acoustic pressure transmission coefficient t_{p}, the amplitude of acoustic pressure in the normal material can be written as $p_{\mathrm{at}} = t_{\mathrm{p}}p_{\mathrm{ai}}$. Therefore, the acoustic pressure in the normal material can be expressed as $p_{\mathrm{n}}(x) = t_{\mathrm{p}}p_{\mathrm{ai}}\exp(\mathrm{j}k_{\mathrm{n}}(x-7))$, where $k_{\mathrm{n}} = \omega/v_0$ is the wave vector of the medium in the normal material. By combining the expressions for $p_{\mathrm{n}}(x)$ with Eqs. (9) and (10), the forward traveling wave solutions can be obtained as

$$\begin{aligned} p_{\mathrm{mix}}(x) &= p_{\mathrm{m}}(x) + p_{\mathrm{n}}(x) = p_{\mathrm{ai}}^{\mathrm{e}}\,\mathrm{e}^{-k_1 x} + r_{\mathrm{p}}p_{\mathrm{ai}}\,\mathrm{e}^{\mathrm{j}7k}\,\mathrm{e}^{k_1 x} \\ &\quad + t_{\mathrm{p}}p_{\mathrm{ai}}\,\mathrm{e}^{\mathrm{j}k_{\mathrm{n}}(x-7)} \quad (\omega < \omega_{\mathrm{m}}), \end{aligned} \tag{11}$$

$$\begin{aligned} p_{\mathrm{mix}}(x) &= p_{\mathrm{m}}(x) + p_{\mathrm{n}}(x) = p_{\mathrm{ai}}^{\mathrm{e}}\,\mathrm{e}^{\mathrm{j}kx} + r_{\mathrm{p}}p_{\mathrm{ai}}\,\mathrm{e}^{\mathrm{j}7k}\,\mathrm{e}^{-\mathrm{j}kx} \\ &\quad + t_{\mathrm{p}}p_{\mathrm{ai}}\,\mathrm{e}^{\mathrm{j}k_{\mathrm{n}}(x-7)} \quad (\omega \geq \omega_{\mathrm{m}}). \end{aligned} \tag{12}$$

The theoretical curves of the acoustic pressure with respect to distance are plotted in Fig. 6. These show the propagation of acoustic waves in the acoustic metamaterial and normal material for excitation frequencies of 250, 350, 450, 453.7, 465, and 900 Hz. For excitation frequencies below f_{m}, the acoustic waves exponentially decay along the metamaterial, e.g., if $f = 250$ Hz, the black curve in Fig. 6(a) indicates that the amplitude of acoustic pressure decreases about 75% in the first three unit cells. When the excitation frequency is 453.7 Hz ($= f_{\mathrm{m}}$), as shown in Fig. 6(b), the acoustic pressures in the metamaterial and the normal material are close to 0 and 2 Pa, respectively. This is because the acoustic pressure reflection and transmission coefficients are 1 and 2 at this excitation frequency. Care must be taken at this critical frequency point, as the hard boundary condition at the interface of the two materials means that only the static pressure with an amplitude of 2 Pa exists, and in the normal material there is no particle vibration and no acoustic wave propagation. When the excitation frequency is 465 Hz ($= f_1$), the acoustic metamaterial has a near zero effective density and the acoustic impedances are matched between the two materials. Thus, as shown in Fig. 6(c), the acoustic pressures in the metamaterial and normal material have the same amplitude, and the phase change inside the metamaterial is apparently slower than inside the normal material. Moreover, transmission enhancement and energy squeezing are achieved, despite the large geometrical mismatch. These extraordinary capabilities may have very appealing applications in sound squeezing and acoustic interconnects. At a frequency of 900 Hz ($> f_1$), the acoustic pressure in the metamaterial is nine times that in the normal material, as shown in Fig. 6(d). This is in inverse proportion to the cross-sectional areas of the two materials.

Using the same method of FEM as in the preceding section, we simulated the propagation of acoustic waves in the composite system. In this FEM simulation, the normal material had the same length as the metamaterial, which consisted of 20 unit cells. The distributions of acoustic pressure in the acoustic metamaterial and the normal material along the propagation path at frequencies of 250 ($< f_1$), 465 ($= f_1$), and 900 Hz ($> f_1$) are plotted in Fig. 7. From Fig. 7(a), we can see that if the frequency is below f_1, the acoustic wave can only propagate into the first few units and the composite system is opaque, similar to that shown in Fig. 6(a). If the frequency is equal to f_1, the acoustic metamaterial has near zero effective density, as plotted in Fig. 7(b). The acoustic pressures in the two materials have the same amplitudes, and the pressure distribution in the propagation path is the same as that shown in Fig. 6(c). Moreover, as expected, we can see from Fig. 7(b) that the phase changes slowly and the effective wavelength in the metamaterial is much longer than in the normal material. Good transmission and energy squeezing are achieved through the RINZ metamaterial. If the frequency is above f_1, e.g., 900 Hz, the acoustic wave propagates well in the composite system, and the propagation velocity in the two materials is the same, as shown in Fig. 7(c). These simulation results are completely consistent with those obtained in the preceding theoretical analysis.

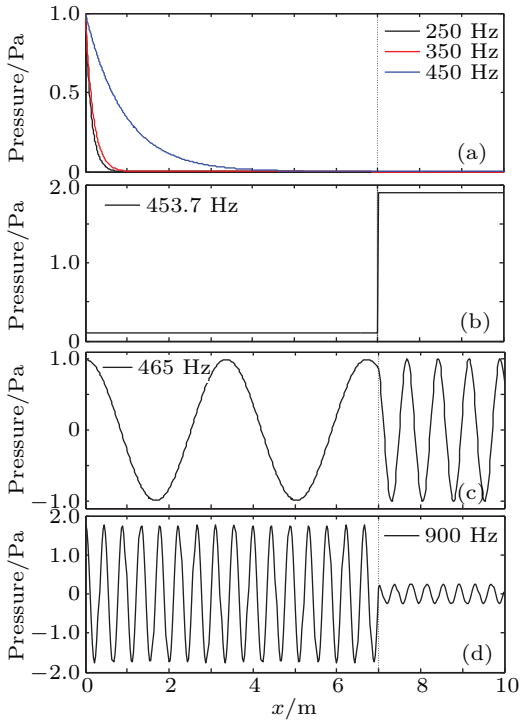

Fig. 6. (color online) Acoustic pressure distributions along the RINZ acoustic metamaterial and normal material with respect to frequency (a) below f_{m}, (b) equal to f_{m}, (c) equal to f_1, and (d) above f_1.

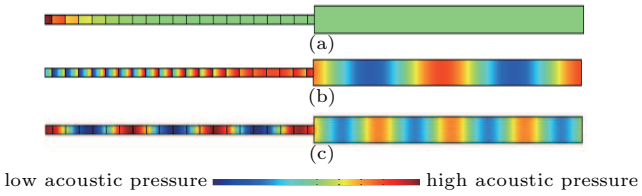

Fig. 7. (color online) FEM simulation results of acoustic pressure field in the composite system at the frequency (a) below, (b) equal to, and (c) above f_1 (465 Hz).

3. Conclusion

In this study, we numerically investigated the characteristics of a RINZ acoustic metamaterial using an interspaced array of membranes. The acoustic properties at two critical frequency points, the resonant frequency f_{m} and the specific frequency f_1, have been discussed for a composite system constructed with the RINZ metamaterial and a normal waveguide material. At the resonant frequency f_{m}, the effective density is zero and the metamaterial exhibits a very low refractive index, the phase velocity becomes very large, and there is little phase variation. These remarkable properties could lead to potential applications in phase couplers, acoustic wave filters, and wave front transformers. At the specific frequency f_1, the effective density is near zero (i.e., the refractive index is near zero), the acoustic impedances of the metamaterial and the normal material are matched, and the distribution of acoustic pressure in the composite system proves that energy squeezing and transmission enhancement are achieved through the RINZ metamaterial. These results provide some new potential opportunities for acoustic applications in a wide range of fields, such as sound squeezing, acoustic interconnectors, and so on.

References

[1] Lee S H, Park C M, Seo Y M, Wang Z G and Kim C K 2009 *Phys. Lett. A* **373** 4464
[2] Fan L, Zhang S Y and Zhang H 2011 *Chin. Phys. Lett.* **28** 104301
[3] Cheng Y, Xu J Y and Liu X J 2008 *Phys. Rev. B* **77** 045134
[4] Fang N, Xi D J, Xu J Y, Ambati M, Srituravanich W, Sun C and Zhang X 2006 *Nat. Mater.* **5** 452
[5] Ding C L and Zhao X P 2009 *Acta Phys. Sin.* **58** 6351 (in Chinese)
[6] Fan L, Ge H, Zhang S Y, Gao H F, Liu Y H and Zhang H 2013 *J. Acoust. Soc. Am.* **133** 3846
[7] Lee S H, Park C M, Seo Y M, Wang Z G and Kim C K 2009 *J. Phys-Condens. Mat.* **21** 175704
[8] Seo Y M, Park J J, Lee S H, Park C M, Kim C K and Lee S H 2012 *J. Appl. Phys.* **111** 023504
[9] Lee S H, Park C M, Seo Y M, Wang Z G and Kim C K 2010 *Phys. Rev. Lett.* **104** 054301
[10] Fan L, Chen Z, Deng Y C, Ding J, Ge H, Zhang S Y, Yang Y T and Zhang H 2014 *Appl. Phys. Lett.* **105** 041904
[11] Yang Z, Dai H M, Chan N H, Ma G C and Sheng P 2010 *Appl. Phys. Lett.* **96** 041906
[12] Qian F, Quan L, Wang L W, Liu X Z and Gong X F 2016 *Chin. Phys. B* **25** 024301
[13] Cummer S A, Popa B I, Schurig D, Smith D R, Pendry J, Rahm M and Starr A 2008 *Phys. Rev. Lett.* **100** 024301
[14] Farhat M, Guenneau S and Enoch S 2009 *Phys. Rev. Lett.* **103** 024301
[15] Cheng Y, Yang F, Xu J Y and Liu X J 2008 *Appl. Phys. Lett.* **92** 151913
[16] Li Y and Engheta N 2014 *Phys. Rev. B* **90** 201107
[17] Silveirinha M and Engheta N 2006 *Phys. Rev. Lett.* **97** 157403
[18] Edwards B, Alu A, Young M E, Silveirinha M and Engheta N 2008 *Phys. Rev. Lett.* **100** 033903
[19] Wu Y and Li J C 2013 *Appl. Phys. Lett.* **102** 183105
[20] Wang T T, Luo J, Gao L, Xu P and Lai Y 2014 *Appl. Phys. Lett.* **104** 211904
[21] Park C M and Lee S H 2013 *Appl. Phys. Lett.* **102** 241906
[22] Bongard F, Lissek H and Mosig J R 2010 *Phys. Rev. B* **82** 094306
[23] Fleury R and Alu A 2013 *Phys. Rev. Lett.* **111** 0555501
[24] Fleury R, Sieck C F, Haberman M R and Alu A 2012 *Proceeding of the 164th Meeting of the Acoustical Society of America*, October 22–26, 2012 Kansas City, Missouri
[25] Jing Y, Xu J and Fang N X 2012 *Phys. Lett. A* **376** 2834
[26] Lee S H and Wright O B 2016 *Phys. Rev. B* **93** 024302
[27] Blackstock D T 2000 *Fundamentals of Physical Acoustics* (New York: John Wiley and Sons)